# Cargo induces retromer-mediated membrane remodeling on membranes

Latha Kallur Purushothaman[a] and Christian Ungermann[a,b,*]
[a]Biochemistry Section, Department of Biology/Chemistry, and [b]Center of Cellular Nanoanalytics Osnabrück (CellNanOs), University of Osnabrück, 49076 Osnabrück, Germany

**ABSTRACT** **Endosomes serve as a central sorting station of lipids and proteins that arrive via vesicular carrier from the plasma membrane and the Golgi complex. At the endosome, retromer complexes sort selected receptors and membrane proteins into tubules or vesicles that bud off the endosome. The mature endosome finally fuses with the lysosome. Retromer complexes consist of a cargo selection complex (CSC) and a membrane remodeling part (sorting nexin [SNX]-Bin/amphiphysin/Rvs [BAR], or Snx3 in yeast) and different assemblies of retromer mediate recycling of different cargoes. Due to this complexity, the exact order of events that results in carrier formation is not yet understood. Here, we reconstituted this process on giant unilamellar vesicles together with purified retromer complexes from yeast and selected cargoes. Our data reveal that the membrane remodeling activity of both Snx3 and the SNX-BAR complex is strongly reduced at low concentrations, which can be reactivated by CSC. At even lower concentrations, these complexes still associate with membranes, but only remodel membranes in the presence of their specific cargoes. Our data thus favor a simple model, where cargo functions as a specific trigger of retromer-mediated sorting on endosomes.**

**Monitoring Editor**
Jean E. Gruenberg
University of Geneva

Received: Jun 4, 2018
Revised: Jul 30, 2018
Accepted: Aug 29, 2018

## INTRODUCTION

Organelles of the endomembrane system are in constant exchange of membranes and proteins via vesicular and tubular carriers. Formation of these carriers involves cargo sorting and concentration, membrane deformation, and, finally, pinching off from their donor membrane to fuse with the target organelle (Gomez-Navarro and Miller, 2016). Organelles are thus confronted with a constant dynamic flux of membrane and volume (Heinrich and Rapoport, 2005). This is particularly apparent for endosomes, which receive cargo via endocytic vesicles from the plasma membrane as well as via Golgi-derived vesicles (Huotari and Helenius, 2011). The constant influx of membrane and volume coincides with the sorting of membrane proteins into intraluminal vesicles (ILVs), which bud into the endosomal lumen, as well as for the recycling of proteins and lipids back to the donor organelles (Henne *et al.*, 2011). During this process, endosomes change their shape from an organelle with multiple tubular extensions to a round organelle with multiple ILVs, which is named multivesicular body or late endosome (Klumperman and Raposo, 2014). On fusion with the lysosome, ILVs are degraded in the lumen by lysosomal hydrolases, and the resulting macromolecules (amino acids, lipids, carbohydrates) are released from the lysosome for reuse.

Membrane remodeling at the endosome requires several protein complexes. Endosomal complexes required for transport (ESCRTs) function in a consecutive order in ILV formation and budding to recognize and sort ubiquitinated membrane proteins that arrive via the endocytic pathway (Henne *et al.*, 2011). The retromer complexes are required for sorting receptor proteins into retrograde transport pathways. Some receptors function as transporters, such as the mannose-6-phosphate receptor, which interacts with glycosylated lysosomal hydrolases at the *trans*-Golgi network (Seaman, 2012). Owing to the acidification of endosomes, the ligand is released from its receptor, which is then sorted back to the Golgi complex through a retromer-dependent pathway (Sorkin and Zastrow, 2009; Seaman, 2012; Burd and Cullen, 2014).

Retromer consists of a trimeric cargo selective complex (CSC) and a second complex, composed of proteins of the sorting nexin family. The CSC consists of Vps35, Vps26, and Vps29 and recognizes specific cargoes. Sorting nexins bind via their

This article was published online ahead of print in MBoC in Press (http://www.molbiolcell.org/cgi/doi/10.1091/mbc.E18-06-0339) on September 6, 2018.
*Address correspondence to: Christian Ungermann (cu@uos.de).
Abbreviations used: BAR, Bin/amphiphysin/Rvs; ESCRT, endosomal complexes required for transport; GDP, guanosine diphosphate; GTP, guanosine triphosphate; IPTG, isopropylthiogalactoside; PMSF, phenylmethylsulfonyl fluoride; RFP, red fluorescent protein; SNX, sorting nexing; YPD, yeast peptone dextran.

Phox-homology (PX) domain to the endosomal lipid phosphatidyl-inositol-3-phosphate (PI-3-P). Snx3 consists only of a PX-domain and forms a distinct complex with the CSC, named Snx3-retromer (Strochlic *et al.*, 2007; Harterink *et al.*, 2011; Burd and Cullen, 2014). Other SNX proteins act as a dimer, such as the SNX-BAR complex, a heterodimer formed by Snx1 (or Snx2) and Snx5 (or Snx6) in metazoan cells, and Vps5 and Vps17 in yeast (Burd and Cullen, 2014). The subunits of this complex have central BAR domains, which form an antiparallel banana-like structure, and are able to deform membranes into long tubules, both in vitro and in vivo (Pylypenko *et al.*, 2007; van Weering *et al.*, 2012a,b; Chi *et al.*, 2014; Daumke *et al.*, 2014; Purushothaman, Arlt, *et al.*, 2017).

On endosomes, retromer binds to the endosomal Rab7 protein, both in yeast and metazoan cells (Rojas *et al.*, 2008; Seaman *et al.*, 2009; Balderhaar, Arlt, *et al.*, 2010; Liu *et al.*, 2012). Rab7 belongs to the group of small lipidated GTPases that can be either in the inactive GDP-bound or the active GTP-bound state (Barr, 2013; Goody *et al.*, 2017). Only if bound to GTP does Rabs interact with their effectors such as retromer. Previous studies have shown that Rab7 and Snx3 binding stabilizes the CSC on membranes (Harrison *et al.*, 2014) and that CSC and Snx3 together form a binding site for cargo, which is formed at the interface of Snx3 and the Vps26 subunit of the CSC (Lucas *et al.*, 2016). Importantly, the addition of a specific cargo strongly facilitated the recruitment of CSC when Rab7 and Snx3 were present in substoichiometric amounts on liposomes (Harrison *et al.*, 2014), suggesting that multivalent interactions facilitate retromer recruitment to membranes.

In previous analyses, we and others showed how the yeast Rab7 protein Ypt7 functions both in the fusion of endosomes with vacuoles and also in retromer recruitment to endosomes (Balderhaar, Arlt, *et al.*, 2010; Liu *et al.*, 2012; Purushothaman, Arlt *et al.*, 2017). Our data revealed that the yeast SNX-BAR retromer can assemble from two subcomplexes, the Ypt7-bound CSC and the PI-3-P interacting SNX-BAR complex. Assembly of the SNX-BAR retromer displaced Ypt7, which could then recruit the fusion machinery. Here, we addressed the role of cargo in carrier formation and provide evidence that cargo can not only be a specific factor to recruit retromer as suggested (Harrison *et al.*, 2014) but also act as an important inducer of the membrane remodeling activity of retromer complexes.

## RESULTS

### Purification of SNX-BAR complexes with membrane remodeling activity

We previously used giant unilamellar vesicles (GUVs) to monitor both the overall activity of the SNX-BAR complex and the recruitment of CSC into the SNX-BAR retromer complex (Purushothaman, Arlt, *et al.*, 2017). To monitor both SNX-BAR and CSC, we tagged Vps17 (SNX-BAR) or Vps29 (CSC) with mGFP or red fluorescent protein (RFP) and purified the resulting complexes via the tandem affinity purification (TAP) tag from yeast (Figure 1A). Tagging did not interfere with assembly, and all complexes showed equal stoichiometry in their subunits. To monitor the activity of the SNX-BAR complex, we added either GFP-tagged or untagged complex to PI-3-P containing membranes, which resulted in a dose-dependent increase in observable tubules emanating from the GUV surface (Figure 1, B and D). Addition of 5–30 nM SNX-BAR induced tubules only on 5-15% of the GUVs, whereas 100 nM induced tubule formation on all GUVs. This activity was similar with GFP-tagged SNX-BAR complex (Figure 1C).

### SNX-BAR retromer assembly induces membrane remodeling

As shown in numerous studies, BAR domains can shape and tubulate membranes in vivo and in vitro (Peter *et al.*, 2004; Frost *et al.*, 2009; van Weering *et al.*, 2012a). In endocytosis, BAR domain proteins induce sequential bending of membranes to form an endocytic vesicle (Daumke *et al.*, 2014; Antonny *et al.*, 2016), a principle that will likely also apply for retromer. On endosomes, the SNX-BAR heterodimer functions together with the CSC, suggesting that the overall ability of the BAR domain to shape membranes is controlled by the assembly of the SNX-BAR retromer and the presence of cargo. To address whether this is indeed the case, we reduced the amount of the GFP-tagged SNX-BAR complex on membranes until no tubulation was observed (Figure 2A). RFP-tagged CSC did not bind to membranes unless SNX-BAR was present (Figure 2, B and C). Addition of 30 nM SNX-BAR to GUVs efficiently sequestered CSC yet did not tubulate GUV-membranes under the selected conditions and with the complex used for this series (Figure 2, C and E). However, when we increased the concentration of CSC in this assay from 10–30 nM, we again observed tubulation on at least 20% of the GUVs. Without CSC, significantly less tubulation was observed in parallel experiments, indicating that CSC has the ability to promote tubule formation of the SNX-BAR complex (Figure 2, D and E). This suggests that assembly of the SNX-BAR retromer can control membrane remodeling via the BAR domain.

### Cargo can be limiting for SNX-retromer membrane remodeling activity

Endosomes contain numerous membrane proteins that need to be sorted back to the plasma membrane or Golgi (Cullen, 2008). One plausible model would be that cargo sequesters CSC to membranes and thereby induces the membrane remodeling activity of the SNX-BAR retromer. We therefore selected concentrations of the SNX-BAR complex and CSC that were insufficient to trigger tubulation yet permitted CSC membrane binding (Figure 3B). We here used non-GFP tagged SNX-BAR complex, which has the same activity as the GFP-tagged complex (Figure 1, B and C). As cargo, we used purified Atto488-labeled His-tagged Vps10, which was then detected in the green channel (see *Materials and Methods*; Figure 3A). GUVs containing the lipid 1,2-dioleoyl-*sn*-glycero-3-[(*N*-(5-amino-1-carboxypentyl) iminodiacetic acid) succinyl] (DOGS-NTA) efficiently sequestered His-Vps10 to the membrane surface (Figure 3C). Strikingly, addition of the cargo protein His-Vps10 to GUVs was sufficient to induce tubulation at concentrations of SNX-BAR (30 nM) and CSC (10 nM) (Figure 3D) that do not result in tubulation otherwise (Figure 3, A and B). Likewise, we observed little SNX-BAR induced tubulation, if just cargo was added (Figures 3, C and H, and 1D). Importantly, addition of Pep12, a cargo of the Snx3-retromer, had no effect on SNX-BAR retromer mediated tubulation (see Figure 6C later in this article).

To monitor initial phases of cargo-induced membrane remodeling, we performed the same experiment (Figure 3D), yet 1) lowered the concentration of SNX-BAR and CSC to 5 nM each and 2) reduced the cargo concentration on GUVs from 100–30 nM (Figure 3, E–G). We now observed patches on GUVs, where CSC accumulated and detected it together with cargo on membrane tubules (Figure 3F). Such regions may represent microcompartments on the GUV membrane, where SNX-BAR retromer complexes assemble as a coat together with its cargo. At higher concentrations of CSC (10 nM), multiple tubules were observed on at least 35% of the GUVs (Figure 3, G and H). In the absence of CSC, we observed little SNX-BAR induced tubulation (Figures 3, C and H, and 1D), consistent with the relocalization of Vps10 to vacuoles on CSC deletion (Seaman *et al.*, 1997). Our data thus suggest that cargo on membranes can serve as a nucleation point of CSC recruitment, SNX-BAR retromer assembly, and subsequent membrane remodeling.

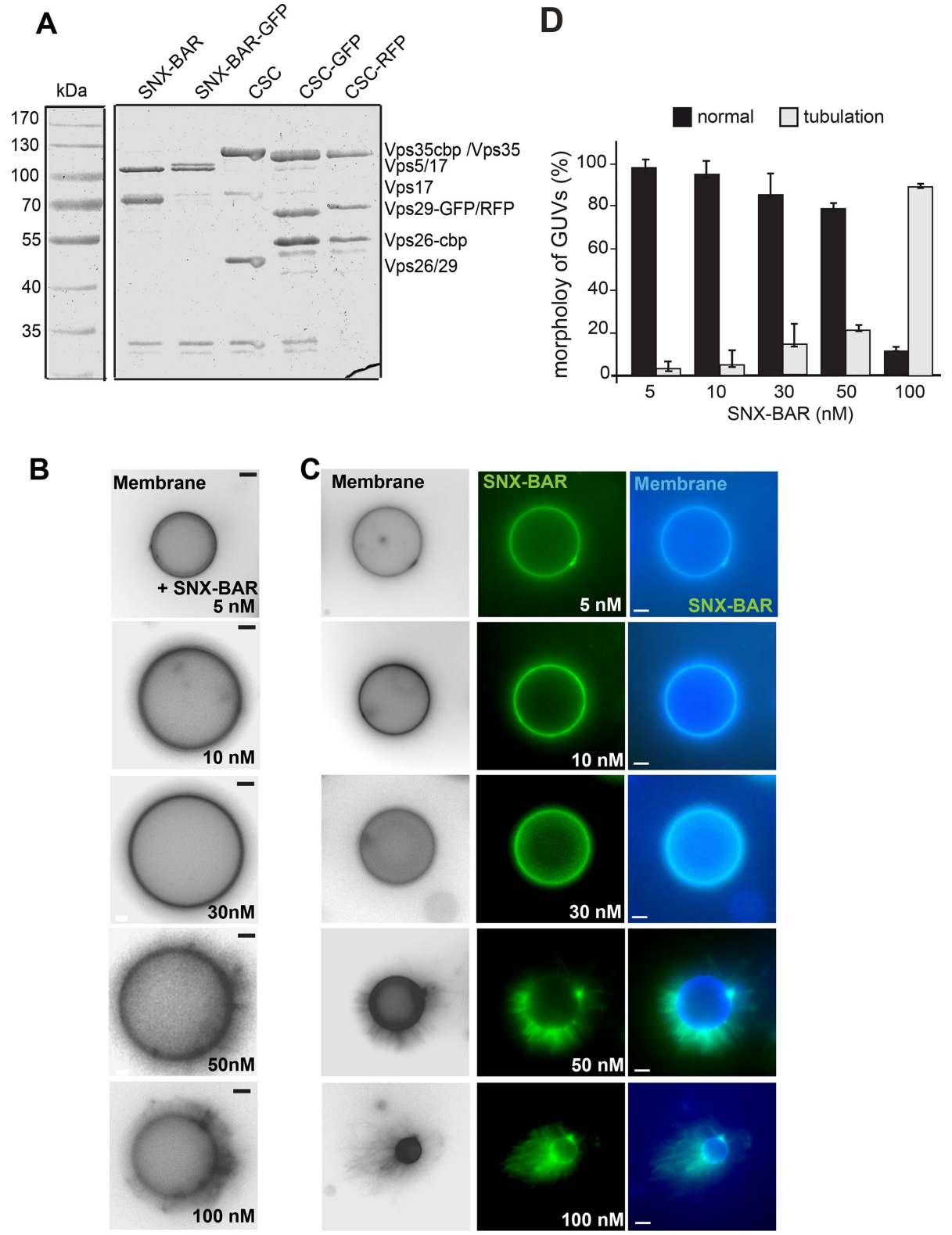


FIGURE 1: Concentration-dependent membrane deformation by SNX-BAR proteins. (A) Purification of all proteins used in this study. Retromer subcomplexes with and without the indicated fluorescent tag were purified as described in *Materials and Methods*. (B, C) Membrane deformation by the Vps5-17 SNX-BAR dimer. The indicated amount of purified SNX-BAR complex without (B) or with (C) Vps17-GFP were titrated to GUVs at the indicated concentration in a 30-µl reaction volume, incubated for 15 min at room temperature, and then analyzed by fluorescence microscopy. Membranes were stained with Marina Blue DHPE lipid dye. Images of membranes were converted to black and white for better visualization. (D) Quantification of the tubulation by the tagged SNX-BAR complex. Data are represented as mean ± SD of three independent experiments. For details see *Materials and Methods*. Scale bar, 5 µm.

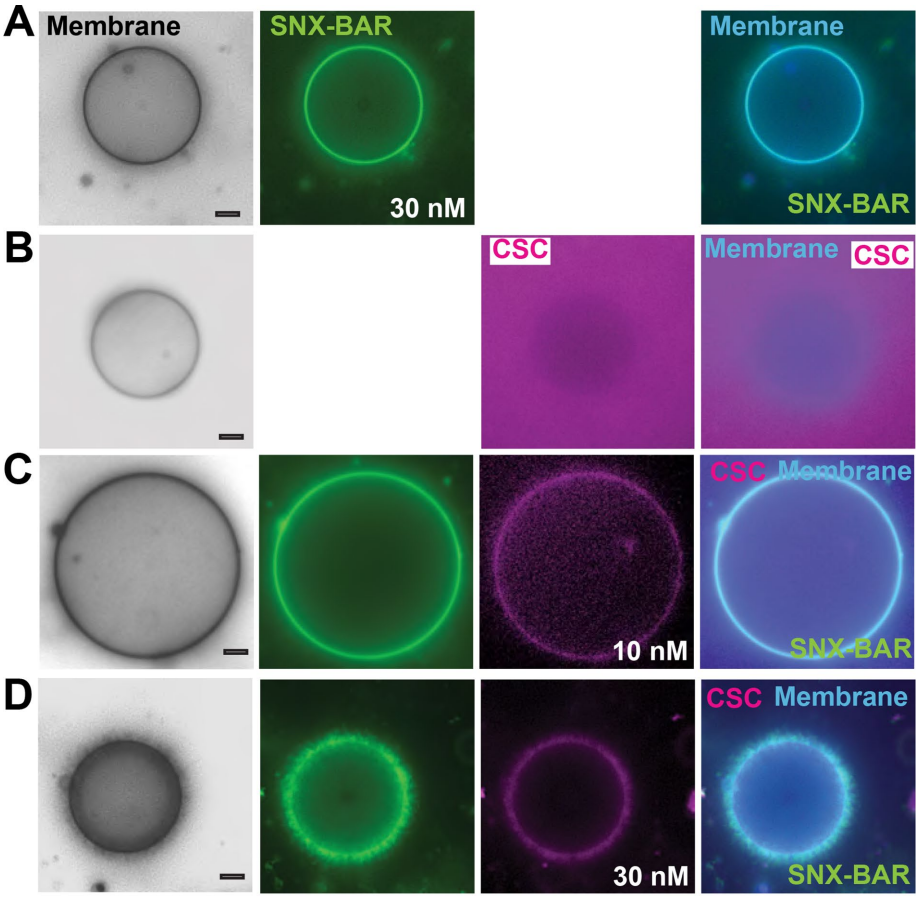


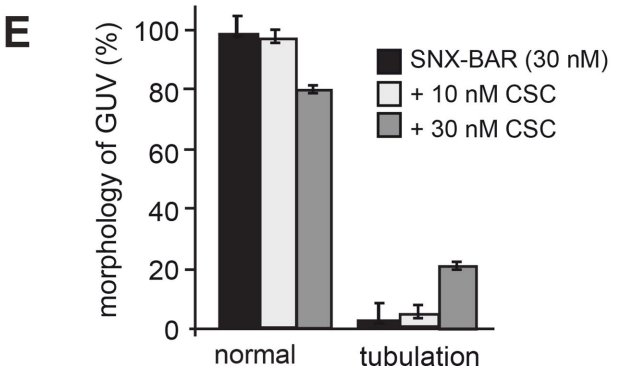


FIGURE 2: CSC can stimulate membrane-deformation activity of the SNX-BAR protein complex. (A) Control of SNX-BAR protein on membranes. Purified GFP-tagged SNX-BAR complex (30 nM) was added to GUVs and analyzed as in Figure 1C. (B) CSC has no affinity for membranes. Limiting amounts of CSC (30 nM) were incubated with the GUVs in the absence of the SNX-BAR complex. (C, D) Titration of CSC to SNX-BAR–bearing membranes. The indicated amounts of RFP-tagged CSC (Vps29-RFP) was added to membranes together with the previously (in A) determined amount of GFP-tagged SNX-BAR complex. GUV membranes were stained as in Figure 1B. (E) Quantification of the results. Tubulation was quantified as described under *Materials and Methods*. Data are represented as mean ± SD. Scale bar, 5 μm. Note that under the selected conditions, 30 nM of SNX-BAR had very little effect on membrane tubulation here.

## CSC can control activity of the Snx3 on membranes

To analyze whether this model applies also to other retromer complexes, we turned to the Snx3 retromer complex. Snx3 is required for the recycling of Pep12, which accumulates on the vacuole in its absence (Figure 4A) (Hettema *et al.*, 2003). As shown before for retromer-dependent Vps10 recycling (Arlt *et al.*, 2015b), transiently overexpressed GFP-tagged Pep12 only distributed into endosomal dots in wild-type cells but not if either Snx3 or the CSC subunit Vps35 were lacking, further confirming that Snx3 and Vps35 function together in Pep12 sorting (Figure 4B).

We next purified Snx3 or mGFP-tagged Snx3 as a His-tagged protein from bacteria (Figure 4C). To test its activity on membranes, we added either of the two proteins to PI-3-P containing membranes. At high concentrations (100 nM), Snx3-GFP caused membrane remodeling, which required PI-3-P on membranes (Figure 3D). Even though Snx3 has an N-terminal His-tag, the presence of DOGS-NTA in GUVs was not sufficient for its membrane recruitment (Figure 4D). We noticed, however, that omission of DOGS-NTA resulted in very poor recruitment of Snx3 to membranes (not shown), suggesting that PI-3-P binding is necessary but possibly not sufficient for its localization to liposomes. It is likely that the endosomal localization of Snx3 requires cargo or another factor apart from PI-3-P.

To monitor sequential steps in Snx3 activity, we titrated Snx3-GFP to GUVs. At low concentrations of 5 nM, Snx3-GFP was distributed over the surface. When we used 15 nM, Snx3-GFP concentrated in patches. However, at higher concentrations of 30–100 nM, Snx3-GFP induced large vesicles blebbing on the GUV membranes (Figure 4E). This activity was not due to the GFP tag as untagged Snx3 also functioned efficiently (Figure 4, F vs. G). We thus conclude that Snx3 is a membrane-active protein under the selected conditions, which can induce membrane deformations.

We again selected the lowest Snx3 concentration, which does not result in membrane deformation and asked whether sequential titration of CSC would be sufficient to trigger membrane remodeling. At low concentrations (5 nM), CSC was recruited to the Snx3-decorated membrane (Figure 5A). When we then increased CSC concentration, we observed formation of Snx3- and CSC-positive patches (Figure 5B), which eventually caused membrane deformation on up to 25% of the GUVs (Figure 5, C and D). We consider it most likely that Snx3 and CSC form a 1:1 complex as published (Lucas *et al.*, 2016), though its formation (and possible oligomerization) on membranes may require an excess of CSC to facilitate the formation during our experimental analysis. In agreement, the detection of the complex between Snx3 with CSC in vivo also required the use of a cross-linker (Strochlic *et al.*, 2007). Our data suggest that CSC promotes Snx3 activity, possibly by a local concentration of Snx3-retromer assembly and polymerization.

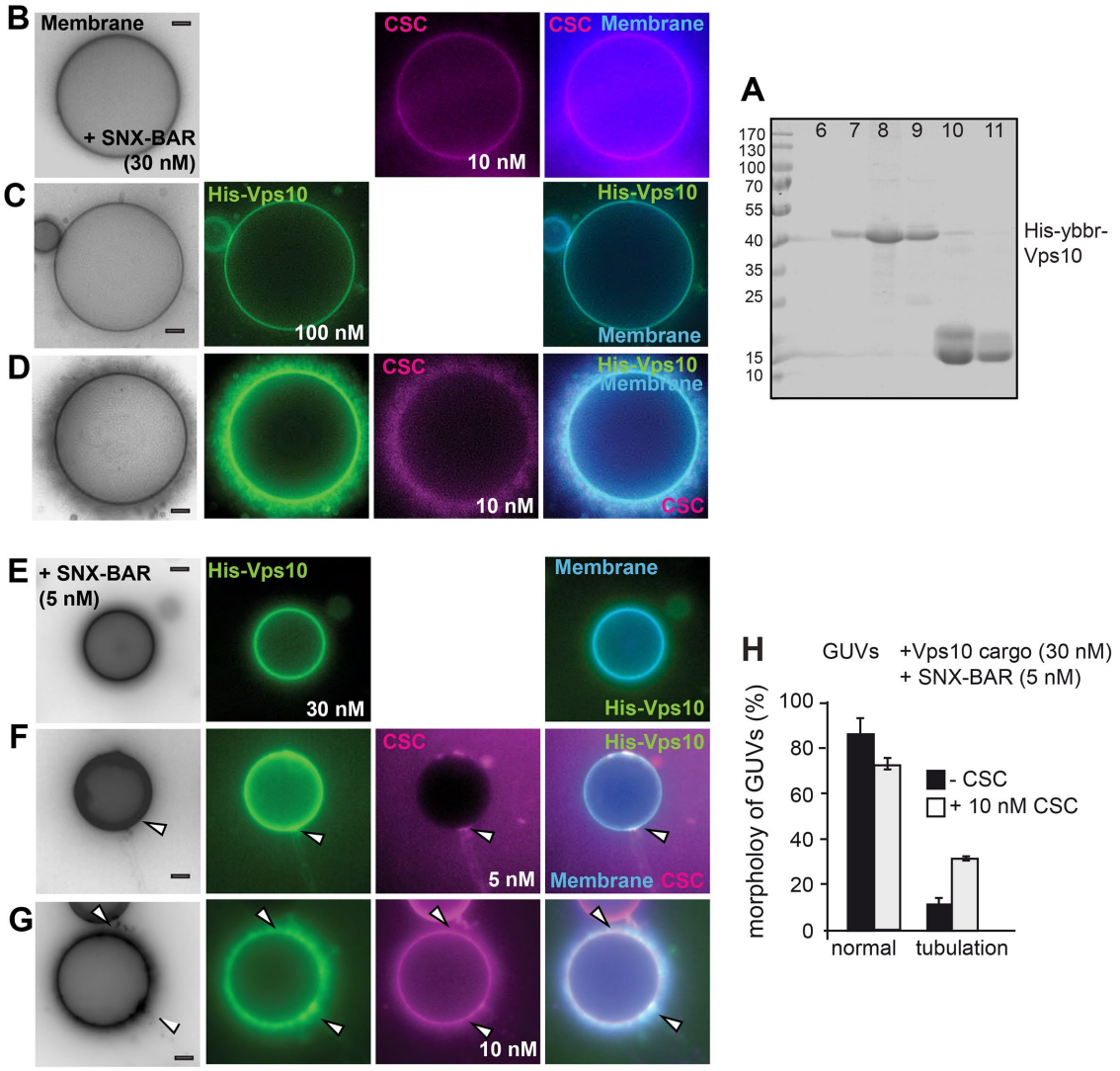


FIGURE 3: Cargo can induce SNX-BAR retromer activity on membranes. (A) Purification of the cytosolic domain of Vps10 via size-exclusion chromatography. His-YbbR-Vps10, corresponding to the cytosolic domain (amino acids 1416–1579), was purified by NTA-purification (see *Materials and Methods*), and the eluate was then loaded onto a Superdex 75 column. Fractions were collected, and samples of peak fractions were added to SDS–sample buffer, boiled, and analyzed by SDS–PAGE and Coomassie staining. (B) GUV morphology in the presence of limiting amount of retromer. The indicated amount of non GFP-tagged SNX-BAR and RFP-tagged CSC complexes were added to GUVs and analyzed as before. (C) Recruitment of Vps10 to GUVs. The cytosolic domain of labeled His-tagged Vps10 was incubated with DOGS-NTA containing GUVs at room temperature for 20 min, then SNX-BAR complex (30 nM) was added, and images were taken 15 min later. (D) Effect of Vps10 on SNX-BAR retromer. Experiment was done as in C with the same concentration of SNX-BAR (30 nM) and CSC (10 nM) as in A. (E–G) Initial events of cargo-driven membrane deformation. The same incubation as in C and D were repeated with reduced amount of SNX-BAR, CSC, and Vps10. (E) SNX-BAR (5 nM) and Vps10 (30 nM) were incubated with GUVs. (F, G) Effect of CSC on tubulation. The indicated increasing concentrations of CSC (5, 10 nM) were added to the reaction. Arrows indicate events of membrane deformation. Membranes were labeled with marina blue-DHPE as in Figure 1. (H) Quantification of Vps10-loaded tubules in the absence or presence of CSC (10 nM) as observed in G. Quantification of tubules from cargo-loaded GUVs in the presence or absence of CSC. Data are represented as mean ± SD. Scale bar, 5 μm.

### Cargo can promote Snx3-retromer activity

To address the effect of cargo on the Snx3-retromer, we purified the cytoplasmic domain of Pep12, resolved it by gel filtration (Figure 6A), labeled it at the N-terminal ybbR-tag with Atto647, and removed the His tag afterward, which prevented membrane binding (Figure 6B). To determine whether Pep12 is a substrate of Snx3, we used His-tagged Snx3 without the C-terminal GFP tag (Figure 4C), which has activity similar to the GFP-tagged Snx3 (Figure 4, F and G). We then added low concentrations of Snx3 (5 nM) and observed Pep12 (here at 10 nM) in distinct spots on the GUV membrane (Figure 6C). This suggests that Snx3 itself has some specificity for Pep12.

To analyze whether cargo can trigger Snx3-retromer activity on membranes, we followed a similar approach as for the SNX-BAR retromer analysis (Figure 3). We therefore added a larger amount of Pep12 (100 nM, compared with 10 nM in Figure 6C) together with low concentrations of Snx3 and CSC to GUVs, which are insufficient

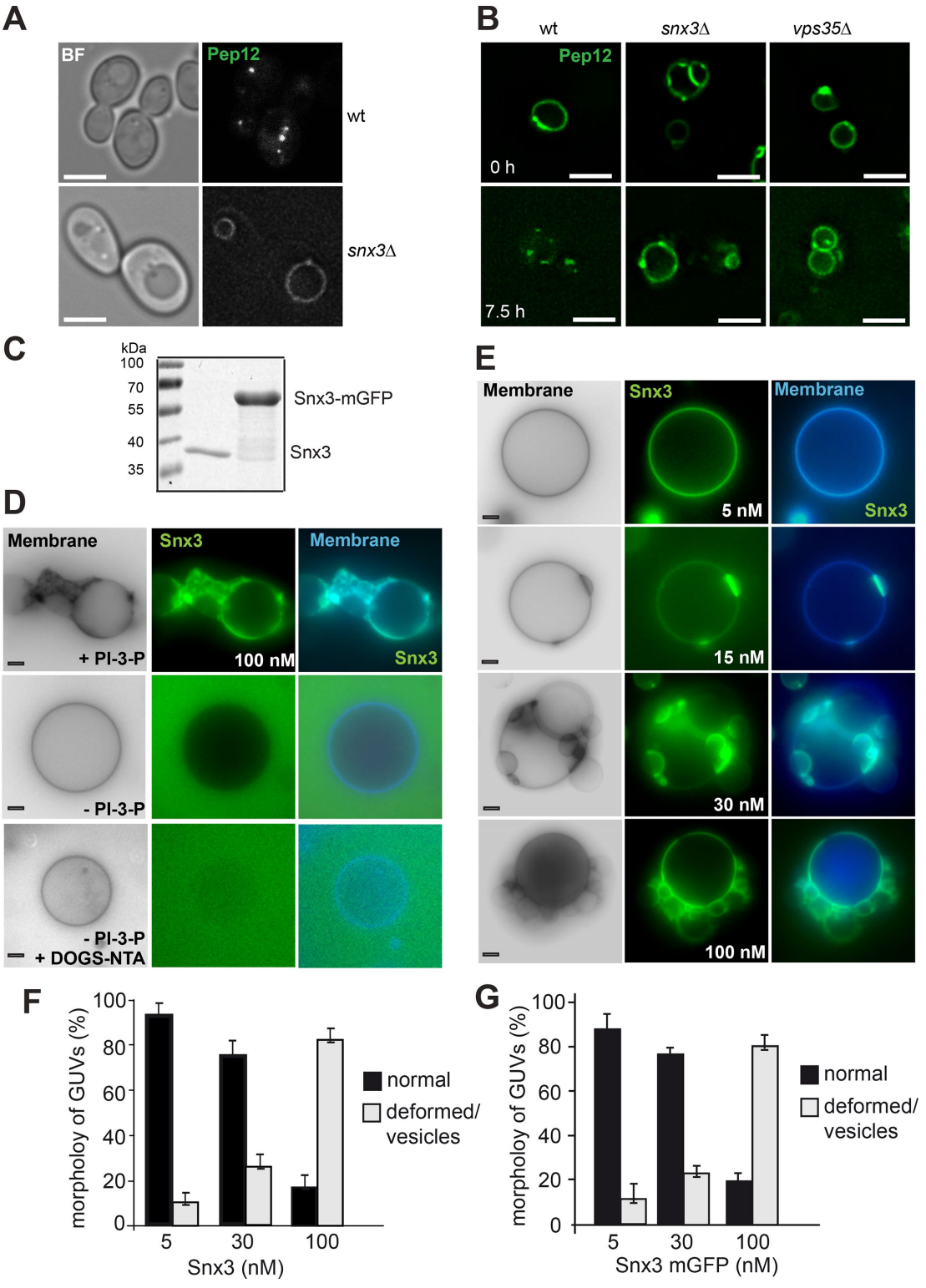


FIGURE 4: SNX3 vesiculates membranes. (A) Localization of the Snx3 cargo Pep12 in cells. Wild-type (wt) and *snx3*Δ cells expressing GFP-tagged Pep12 were analyzed by fluorescence microscopy. (B) Recycling of Pep12 from vacuoles requires Snx3 and CSC. GFP-Pep12 was overexpressed from the *GAL1* promoter in wild-type, *snx3*Δ, and *vps35*Δ cells. Cells grown in log-phase were shifted to glucose containing yeast peptone dextran (YPD) medium and analyzed by fluorescence microscopy at the indicated time points. (C) Purified Snx3 and Snx3-GFP (see *Materials and Methods*) were analyzed by SDS–PAGE and Coomassie staining. (D) Membrane activity of Snx3 depends on PI-3-P. GUVs were made with or without PI-3-P or DOGS-NTA, stained with marina blue DHPE, and incubated with 100 nM Snx3-mGFP for 15 min before being analyzed by fluorescence microscopy. (E) Titration of Snx3-GFP to GUVs containing PI-3-P and DOGS-NTA. The indicated amounts were added and GUVs were analyzed as in D and quantified (F). Quantification of non GFP-tagged Snx3-induced membrane deformation is shown in G. Data are represented as mean ± SD. Scale bar, 5 μm.

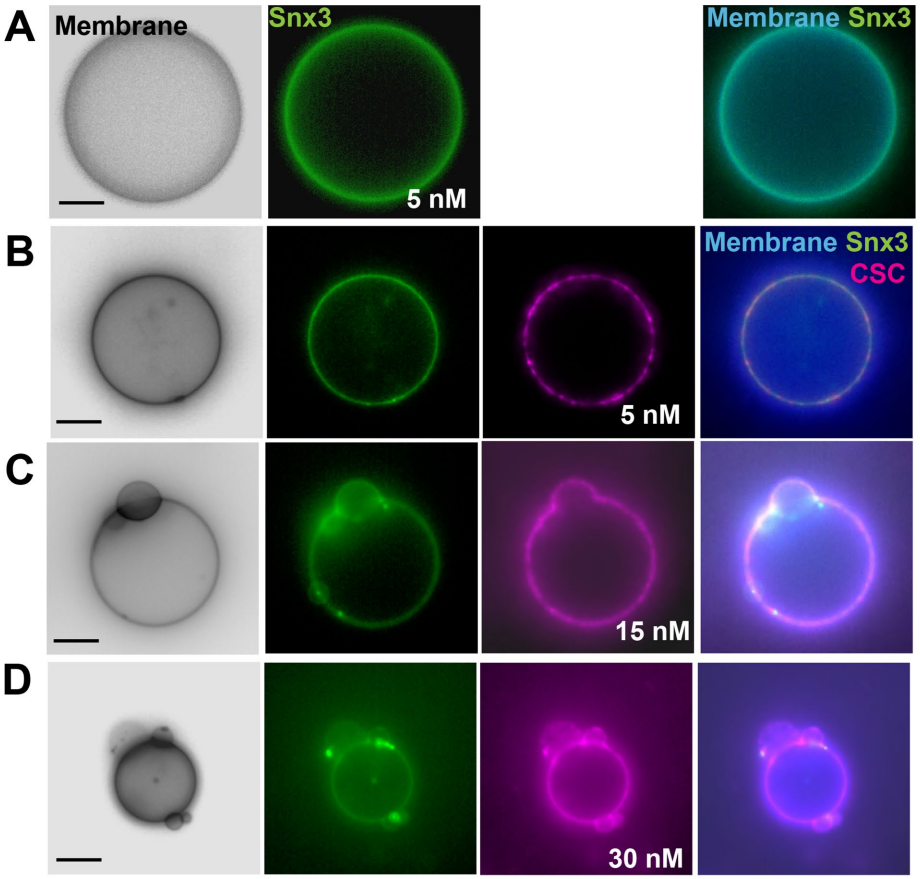


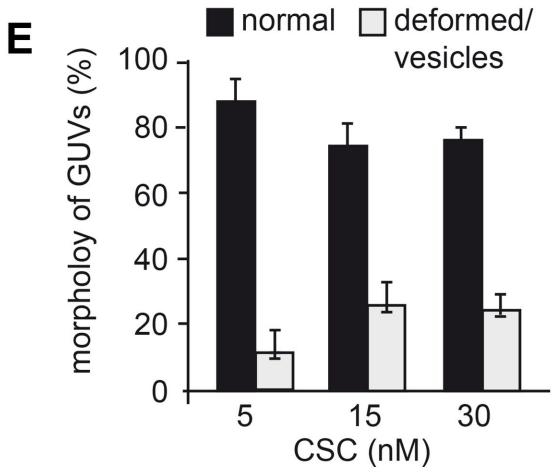


FIGURE 5: CSC can trigger Snx3-driven membrane deformation. (A–D) Limiting amounts of Snx3-mGFP (5 nM) were added alone (A) or together with increasing amounts of CSC (5–30 nM, B–D) to GUVs as in Figure 3, incubated for 15 min, and then examined by fluorescence microscopy. (E) Quantification of vesiculation in the presence of SNX3-mGFP at the indicated amounts of CSC. The quantification of Snx3-GFP induced deformation is the same as in Figure 4G and is shown here for comparison. Data are represented as mean ± SD. Scale bar, 5 µm.

to deform membranes on their own (Figure 6D). As for the SNX-BAR retromer (Figure 3), cargo triggered retromer-dependent membrane deformation on up to 40% of all GUVs (Figure 6, D and H). As mentioned above, SNX-BAR and CSC did not sequester the Pep12 cargo to GUVs, in agreement with Pep12 being a specific cargo of Snx3 (Figure 6E) (Hettema *et al.*, 2003). Importantly, the binding of Pep12 was specific; Vps10 as a cargo of SNX-BAR retromer did not trigger Snx3-retromer mediated membrane deformation (Figure 6F). These observations show that Pep12 as a specific cargo protein can trigger Snx3-retromer activity to remodel membranes.

To monitor early events in the assembly of cargo with Snx3-retromer, we followed colocalization of CSC and the Pep12 cargo (Figure 6G). We again selected low Pep12 cargo concentrations of 10 nM compared with our initial analysis with 100 nM, reasoning that we would then possibly resolve separate events of cargo-induced retromer activation (Figure 6D). Only in the presence of both Snx3 and CSC were multiple distinct events of membrane deformation observed: Pep12 and CSC either accumulated in patches proximal to deformed membranes (Figure 6G, a and b) or were present in the deformed structures (Figure 6Gc). These events were strongly reduced in the absence of CSC (Figure 6, C and H).

Unlike for the His-tagged Vps10 as a substrate of SNX-BAR (Figure 3), the Pep12 does not contain a His tag. The cargo Pep12 therefore required Snx3 and CSC for its recruitment to the GUV membrane (Figure 6, C and D) rather than itself sequestering the Snx3-retromer to membranes. This strongly suggests that cargo is in our experimental setup not just another binding site for the Snx3-retromer on membrane. Our data rather imply that cargo can activate the Snx3-retromer complex to deform membranes.

## DISCUSSION

Our data provide a mechanistic explanation of how the activity of retromer complexes is controlled on endosomes. We show that the SNX proteins can be limiting for tubule formation. Assembly together with the CSC complex results in a local concentration, presumably by assembling multiple retromer complexes into structures that eventually deform the membrane. With even lower SNX and CSC concentrations, the entire reaction becomes dependent on the presence of cargo (Figures 3 and 6). Cargo may then either 1) induce polymerization of SNX-retromer complexes or 2) recruit further complexes to the endosome, which then promotes assembly. At least for Snx3, our data suggest the former possibility because soluble cargo triggered membrane deformation (Figure 6G).

As retromer complexes are cargo specific (Strochlic *et al.*, 2007; Harterink *et al.*, 2011; Steinberg *et al.*, 2013; Burd and Cullen, 2014), we speculate that cargo binding also enables them to interact with each other. Their assembly should result in distinct membrane domains with unique identity. Indeed, SNX-BAR retromer complexes have been detected in tubular structures together with cargo (van Weering *et al.*, 2012b; Chi *et al.*, 2014; Arlt *et al.*, 2015a;

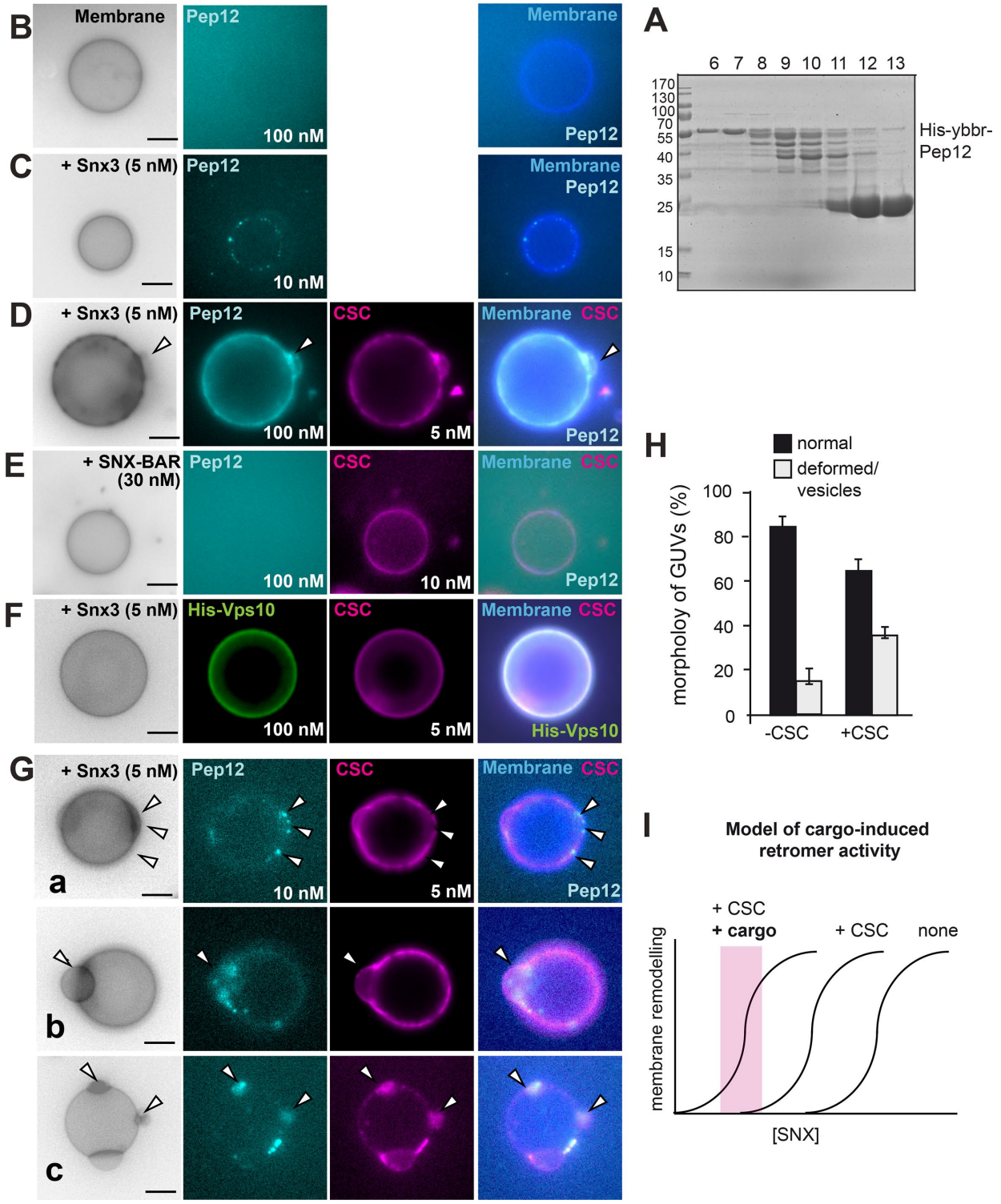


FIGURE 6: Cargo-induced vesiculation and domain formation by the Snx3-retromer. (A–C) Purification and analysis of Snx3 cargo. Purification of the cytosolic domain of Pep12 (A). N-terminally His-tagged Pep12 (amino acids 1–266) was purified via Ni-NTA resin, the His-tag was removed by protease cleavage, and the eluate was applied to a gel-filtration column. Fractions were analyzed by SDS–PAGE and Coomassie staining (see *Materials and Methods*). Fractions 6 and 7 were pooled and labeled as described under *Materials and Methods* and added to GUVs in the absence (B) or presence (C) of non-GFP-tagged Snx3 (5 nM) for 15 min and analyzed by fluorescence microscopy. (D) Pep12 triggers Snx3-retromer membrane remodeling activity. Snx3 and CSC (5 nM each) were added with 100 nM Pep12 to GUVs and analyzed as before. (E) SNX-BAR retromer addition together with Pep12 to GUVs. SNX-BAR complex (30 nM) and CSC (10 nM) were added and analysis was done as in D. (F) Snx3-retromer does not cluster the Vps10 cargo. His-tagged Vps10 (100 nM) was added together with Snx3 (5 nM) and CSC (5 nM) to GUVs. (G) Early events of cargo-induced membrane deformation by Snx3-retromer. Snx3 and CSC (5 nM each) were added together with 10 nM Pep12 to the

Varandas *et al.*, 2016). This cooperation of retromer complexes with cargo can explain the coordination of multiple sorting events on a single endosome (Klumperman and Raposo, 2014).

Even though we can observe cargo specificity and the induction of membrane remodeling, our reconstitution certainly lacks additional players as both retromer complexes cause global changes in the membrane structures. This could be due to either the composition of the GUV membrane or factors that restrict the expansion of domains and cooperate with SNX-retromer complexes such as the actin cytoskeleton (Seaman *et al.*, 2013). It is furthermore possible that protein crowding and subsequent phase partitioning on the GUV membrane contribute to the formation of the large Snx3-vesicles, very similar to phenomena described before (Stachowiak *et al.*, 2012), whereas the SNX-BAR induced tubules are comparable to structures observed by others and us (van Weering *et al.*, 2012a; Chi *et al.*, 2014; Purushothaman, Arlt, *et al.*, 2017). Once formed, retromer-coated tubules or vesicles need to undergo fission and get transported to their destination. Fission may require a dynamin protein or Atg18 (Chi *et al.*, 2014; Arlt *et al.*, 2015b; Gopaldass *et al.*, 2017), possibly in the context of the actin network (Seaman *et al.*, 2013).

It is well known that membrane localization of retromer depends on Rab7 (Rojas *et al.*, 2008; Seaman *et al.*, 2009). Furthermore, retromer recruits a Rab7 GAP to endosomes and thus controls its activity in vivo (Jimenez-Orgaz *et al.*, 2018). Also yeast Ypt7-GTP can bind to the CSC and recruit it to membranes (Balderhaar, Arlt, *et al.*, 2010; Liu *et al.*, 2012; Purushothaman, Arlt, *et al.*, 2017). To simplify our system, we intentionally omitted Ypt7 from our analyses, as this would have further complicated the dissection of CSC and cargo contribution to SNX-induced membrane deformation. We would like to stress that we have no evidence that CSC itself has a membrane remodeling activity, even if it is bound to membranes via Ypt7 (Purushothaman, Arlt, *et al.*, 2017).

Our data can be incorporated into a revised working model of retromer function on membranes. Endosomes initially receive cargo from the plasma membrane and Golgi. Locally generated PI-3-P, and activated Rabs, most prominently Rab5 and Rab7, then recruit membrane remodeling complexes such as Snx3 and the SNX-BAR dimer. These complexes may not remodel membranes in the absence of cargo, possible due to lower concentrations than necessary for membrane remodeling (Figure 6I), which would be similar to our observations in vitro, when we titrated their concentration down (Figures 1 and 4). The specific cargo can serve either as a nucleation point to assemble the individual Snx3, SNX-BAR, and CSC complexes into multimeric assemblies, which in turn may cause protein crowding and membrane deformation (Stachowiak *et al.*, 2012). Such transitions may be similar to allosteric activation of enzymes as depicted in our working model (Figure 6I), which requires future detailed analyses. Additional factors like Rab7 and PI-3-P, which bind SNX and CSC complexes, will also contribute to this process and allow for further fine-tuning or clustering. Indeed, previous work on Snx3-retromer revealed that Rab7, PI-3-P, and a specific cargo cooperate in retromer recruitment to membranes (Harrison *et al.*, 2014). Cargo-based recognition might similarly direct ESCRT complexes and other Snx-complexes to endosomes. In agreement, we and others were not able to clearly separate ESCRT from retromer function, when tracing endosomes over time (Strochlic *et al.*, 2007; Arlt *et al.*, 2015a), suggesting that available cargo dictates their recruitment and function rather than a consecutive order of retromer and ESCRTs. Interestingly, mammalian SNX-BAR complexes function without CSC to relocalize the mannose-6-phosphate receptor to the Golgi (Kvainickas *et al.*, 2017; Simonetti *et al.*, 2017). At least for yeast Vps10, which functions similarly like the mannose-6-phosphate receptor, the entire SNX-BAR retromer is required for efficient Golgi relocalization in vivo (Seaman *et al.*, 1997; Arlt *et al.*, 2015b). Despite this difference, it is likely that cargo is in either case central inducer of the membrane remodeling activity.

In sum, our data show that assembly with CSC and cargo at the endosome activates sorting nexins, which results in higher membrane remodeling activity. This mechanism can explain how activation of sorting nexins can be controlled by the presence of cargo.

## MATERIALS AND METHODS

### Strains

Yeast strains used in this study are listed in Table 1. All *Saccharomyces cerevisiae* strains were made by genetic manipulation using homologous recombination of overlapping PCR fragment as described previously (Longtine *et al.*, 1998; Janke *et al.*, 2004).

### Plasmid generation

To generate the pET28a-*HIS-SUMO-ybbR-VPS10* plasmid, the coding region for the C-terminal fragment of Vps10 (corresponding to amino acid residues 1416–1579) was amplified by PCR from genomic DNA using Phusion polymerase with primers also encoding the ybbR tag. The PCR fragment was cut with *Bam*HI and *Xho*I and inserted into the digested pET28a-*HIS-SUMO* vector. Similarly, the coding region of the cytosolic domain of Pep12 (corresponding to residues 1–266) was amplified with primers also coding for the ybbR tag and cloned similarly into the pET28a-*HIS-SUMO* vector. To generate an expression plasmid for His-SUMO-tagged Snx3, the Snx3 coding region was PCR amplified from genomic DNA and cloned into a pET28aHis-SUMO vector via *Bam*HI and *Sal*I restriction sites. To generate C-terminally tagged Snx3, the mGFP coding sequence was amplified from a corresponding plasmid and cloned into the pET28a-*HIS-SUMO-SNX3* background vector via *Sal*I and *Not*I, while removing the C-terminal stop codon.

### Protein purification

Recombinant proteins were purified from *Escherichia coli* BL21 (DE3) Rosetta cells expressing plasmid the corresponding plasmids (pET28a-*HIS-SUMO-ybbR-VPS10*, pET28a-*HIS-SUMO-ybbR-PEP12*, pET28a-*HIS-SUMO-SNX3*, or pET28a-*HIS-SUMO-SNX3-mGFP*). Cells were grown at 37°C to $OD_{600}$ = 0.5 and induced with 0.5 mM isopropylthiogalactoside (IPTG) overnight at 16°C while shaking. Cells were harvested and lysed in precooled fluidizer in 50 mM

GUVs. Arrows in examples a–c show distinct events of membrane deformation and Pep12-CSC colocalization. (H) Quantification of membrane deformation events by Pep12 (10 nM) and Snx3 (5 nM) in the absence of presence of CSC (5 nM) as observed in C and G. Data are represented as mean ± SD (20–35 GUVs from three independent experiments were analyzed for quantification). Scale bar, 5 µm. (I) Model of cargo-induced retromer activity. Without CSC and cargo, more SNX is needed to remodel membrane. CSC and cargo would lower the needed amount of SNX protein on membrane. Note that the curves do not reflect actual measurements but are models based on the findings. For details see the text.

| Strain | Genotype | Reference |
|---|---|---|
| CUY764 | *MATa his3Δ1 leu2Δ0 met15Δ0 ura3Δ0* | EUROSCARF |
| CUY10016 | *CUY764, PEP12::PHO5pr-yeGFP-NatNT2* | This study |
| CUY11308 | *CUY764, snx3Δ::kanMX PEP12::PHO5pr-yeGFP-natNT2* | This study |
| CUY10004 | *CUY764,VPS35:: mCherry-hphNT1 PEP12pr::GAL1pr- yeGFP-natNT2* | This study |
| CUY10005 | *CUY764, vps35Δ::kanMX PEP12pr:: GAL1pr-yeGFP-natNT2* | This study |
| CUY11309 | *CUY764, snx3Δ::kanMX PEP12pr:: GAL1-yeGFP-natNT2* | This study |
| CUY105 | *MATa his3Δ200 leu2Δ0 met15Δ0 trp1Δ63 ura3Δ0* | EUROSCARF |
| CUY100 | *MATalpha his3Δ200 leu2Δ0 lys2Δ0 met15Δ0 trp1Δ63 ura3Δ0* | EUROSCARF |
| CUY9228 | *CUY105, VPS5pr::GAL1pr-natNT1 VPS17pr:: GAL1pr-kanMX VPS5::TAP-URA3 vps35::HIS3* | Purushothaman *et al.*, 2017 |
| CUY9711 | *CUY764, VPS5pr:: GAL1pr- natNT1 VPS17pr:: GAL1pr-kanMXVPS5::TAP-URA3 vps35::HIS3 VPS17::GFP-hphNT1* | Purushothaman *et al.*, 2017 |
| CUY9495 | *CUY100 VPS26pr:: GAL1pr-HIS3 VPS29pr:: GAL1pr-natNT2 VPS35pr::GAL1pr-hphNT1 VPS35::TAP-kanMX vps5::TRP1 vps17::LEU2* | Purushothaman *et al.*, 2017 |
| CUY9932 | *CUY100, VPS26pr::GAL1pr-HIS3 VPS29pr::GAL1pr-natNT2 VPS35pr::GAL1pr-hphNT1 VPS29::mClover-kan VPS26::TAP-URA3 vps5Δ::TRP1* | Purushothaman *et al.*, 2017 |
| CUY9935 | *CUY100, VPS26pr::GAL1pr-HIS3 VPS29pr::GAL1pr-natNT2 VPS35pr::GAL1pr-hphNT1 VPS29::mRuby-kan VPS26::TAP-URA3 vps5Δ::TRP1* | This study |

**TABLE 1:** Strains used in this study.

Tris-HCl, pH 7.4, 150 mM NaCl, supplemented with 0.05x protease inhibitor cocktail (PIC; 1xPIC; corresponds to 0.1 µg/ml leupeptin, 0.5 mM *o*-phenanthroline, 0.5 µg/ml pepstatin A, 0.1 mM Pefabloc) and 1 mM phenylmethylsulfonyl fluoride (PMSF). Lysates were subjected to centrifugation at 20,000 × *g*, and the resulting supernatant was incubated with prewashed Ni-NTA (nickel-nitriloacetic acid) beads, which were prewashed with lysis buffer containing 20 mM imidazole. After 2 h of incubation at 4°C, beads were centrifuged briefly at 2000 × *g* and washed three times with lysis buffer containing 20 mM imidazole. Proteins were eluted in 300 mM imidazole, 50 mM Tris-HCl, pH 7.4, 300 mM NaCl, 10% glycerol, and applied to a Superdex 75 10/300 GL size exclusion column (GE Healthcare), preequilibrated in 50 mM Tris-HCl, pH 7.4, 300 mM NaCl, 10% glycerol. Peak fractions containing the respective protein were collected, pooled, snap frozen, and stored in aliquots at –80°C.

To remove the His tag from ybbR-Pep12, the protein was eluted protein from beads by addition of the SUMO protease for 2 h on a nutator at room temperature and then subjected to labeling.

### Labeling assay

His-SUMO-ybbR-Vps10 or ybbR-Pep12 (5–15 µM) proteins were subjected to enyzmatic labeling reaction with 5 µM Sfp-MBP (4′-phosphopantetheinyl transferase-maltose binding protein) and coenzyme A tagged to the Flurophore OG-488 and Cy5-647, respectively, in buffer containing 50 mM Tris-HCl, pH 7.4, 150 mM NaCl, 10% glycerol, 1 mM $Mg_2Cl$. The enzymatic labeling reaction was carried out for 1–2 h in the dark at room temperature. To stop the reaction, 15 µM EDTA was added. Proteins were then separated by size exclusion chromatography on a Superdex 75 10/300 GL column (GE Healthcare). Peak fractions were collected, pooled, and controlled for labeling in a Vesa-Doc documentation system (BioRad, Germany). Proteins were further analyzed by SDS–PAGE and Coomassie staining.

### GUV preparations

All the lipids were purchased from Avanti Polar Lipids. The desired lipid mix (2 mM in 500 µl) was made using 1,2-dioleoyl-*sn*-glycerol-3-phosphocholine (71 mol%); 1,2-dioleoyl-*sn*-glycerol-3-phosphoethanol-amine (16 mol%); 1,2-dioleoyl-*sn*-glycerol-3-phospho-l-serine (4.4 mol%); the lipid dye Marina Blue 1,2-dihexadecanoyl-*sn*-glycero-3-phosphoethanolamine (DHPE) (0.7 mol%); 1,2-dioleoyl-*sn*-glycero-3-[(*N*-(5-amino-1-carboxypentyl) iminodiacetic acid) succinyl] (DOGS-NTA, nickel salt; 3 mol%); and PI-3-P (Echelon; diC16; 5 mol%) in chloroform: methanol (2:1). The organic solvent was evaporated, and lipids were resuspended in chloroform:methanol (2:1). Then 3 µl of the lipid mix was spotted onto the indium tin oxide–coated side of the ITO plate and left overnight in a vacuum chamber to evaporate any organic solvent. For GUV electroformation, the conducting sides of ITO glass slides were align to face each and separated with a spacer to create a chamber. To this chamber, 500 µl of 300 mM sucrose solution was added, and plates were connected to a Vesicle Prep Pro (Naion, Munich, Germany) generator for GUV electroformation. After 3 h of electroformation cycles, generated vesicles were sedimented in swing bucket rotor at 100 × *g* for 5 min. GUVs (50 µl) were collected from the bottom and transferred into a new reaction vial, which was filled with 450 µl glucose buffer (1 mM HEPES/KOH, pH 7.4, 267 mM glucose, 1 mM dithiothreitol [DTT]) and mixed gently. The mixture was slowly applied to a new vial containing a 10 µl cushion of equal amounts of glucose buffer and sucrose buffer (1 mM HEPES/KOH, pH 7.4, 240 mM sucrose, 1 mM DTT) at a 1:1 ratio. This vial was centrifuged (100 × *g*, 20 min at 4°C). After the centrifugation, ~480 µl of supernatant was removed, and the GUVs on top of the sucrose cushion were taken up in sucrose buffer to reach a total volume of 50 µl. The final concentration of the GUVs was 0.1 mM.

### GUV membrane deformation assays

As a preparation of the assay 96-well plates were blocked with 5% bovine serum albumin in phosphate-buffered saline (PBS) for 1–2 h and then washed at least three times with PBS. Then, 5 µl of GUVs (10 µM) was incubated with the indicated amount of proteins at room temperature for 15 min in a total volume of 30 µl in PBS. To determine

the effect of cargo proteins (His-Vps10 or untagged Pep12), on retromer and SNX3, the indicated amounts of proteins were preloaded onto GUVs and incubated for 20 min before taking images.

GUVs were imaged on an Olympus IX-71 inverted microscope using 60×/numerical aperture (NA) 1.40 and Insights illumination, a scientific complementary metal-oxide semiconductor camera (PCO), and SoftWoRx software (Applied Precision), and the images were processed in ImageJ.

## ACKNOWLEDGMENTS

We thank Lars Langemeyer and Ayelén González Montoro for critical reading of the manuscript, Florian Fröhlich and Daniel Kümmel for discussions, and Kathrin Auffarth and Angela Perz for excellent technical assistance. This work was supported by the Deutsche Forschungsgemeinschaft (DFG) (SFB 944, Project P11). L.K.P. received support by a Boehringer Ingelheim Fonds Travel Fellowship.

## REFERENCES

Boldface names denote co–first authors.

Antonny B, Burd C, de Camilli P, Chen E, Daumke O, Faelber K, Ford M, Frolov VA, Frost A, Hinshaw JE, *et al.* (2016). Membrane fission by dynamin: what we know and what we need to know. EMBO J 35, 2270–2284.

Arlt H, Auffarth K, Kurre R, Lisse D, Piehler J, Ungermann C (2015a). Spatiotemporal dynamics of membrane remodeling and fusion proteins during endocytic transport. Mol Biol Cell 26, 1357–1370.

Arlt H, Reggiori F, Ungermann C (2015b). Retromer and the dynamin Vps1 cooperate in the retrieval of transmembrane proteins from vacuoles. J Cell Sci 128, 645–655.

**Balderhaar HJK, Arlt H,** Ostrowicz C, Bröcker C, Sündermann F, Brandt R, Babst M, Ungermann C (2010). The Rab GTPase Ypt7 is linked to retromer-mediated receptor recycling and fusion at the yeast late endosome. J Cell Sci 123, 4085–4094.

Barr FA (2013). Review series: Rab GTPases and membrane identity: causal or inconsequential? J Cell Biol 202, 191–199.

Burd C, Cullen PJ (2014). Retromer: a master conductor of endosome sorting. Cold Spring Harb Perspect Biol 6, a016774.

Chi RJ, Liu J, West M, Wang J, Odorizzi G, Burd CG (2014). Fission of SNX-BAR-coated endosomal retrograde transport carriers is promoted by the dynamin-related protein Vps1. J Cell Biol 202, 527.

Cullen PJ (2008). Endosomal sorting and signalling: an emerging role for sorting nexins. Nat Rev Mol Cell Biol 9, 574–582.

Daumke O, Roux A, Haucke V (2014). BAR domain scaffoldsin dynamin-mediated membrane fission. Cell 156, 882–892.

Frost A, Unger VM, de Camilli P (2009). The BAR domain superfamily: membrane-molding macromolecules. Cell 137, 191–196.

Gomez-Navarro N, Miller EA (2016). COP-coated vesicles. Curr Biol 26, R54–R57.

Goody RS, Müller MP, Wu YW (2017). Mechanisms of action of Rab proteins, key regulators of intracellular vesicular transport. Biol Chem 398, 565–575.

Gopaldass N, Fauvet B, Lashuel H, Roux A, Mayer A (2017). Membrane scission driven by the PROPPIN Atg18. EMBO J 36, 3274–3291.

Harrison MS, Hung CS, Liu TT, Christiano R, Walther TC, Burd CG (2014). A mechanism for retromer endosomal coat complex assembly with cargo. Proc Natl Acad Sci 111, 267–272.

Harterink M, Port F, Lorenowicz MJ, McGough IJ, Silhankova M, Betist MC, van Weering JRT, van Heesbeen RGHP, Middelkoop TC, Basler K, *et al.* (2011). A SNX3-dependent retromer pathway mediates retrograde transport of the Wnt sorting receptor Wntless and is required for Wnt secretion. Nat Cell Biol 13, 914–923.

Heinrich R, Rapoport T (2005). Generation of nonidentical compartments in vesicular transport systems. J Cell Biol 168, 271–280.

Henne WM, Buchkovich NJ, Emr SD (2011). The ESCRT pathway. Dev Cell 21, 77–91.

Hettema E, Lewis M, Black M, Pelham H (2003). Retromer and the sorting nexins Snx4/41/42 mediate distinct retrieval pathways from yeast endosomes. EMBO J 22, 548–557.

Huotari J, Helenius A (2011). Endosome maturation. EMBO J 30, 3481–3500.

Janke C, Magiera MM, Rathfelder N, Taxis C, Reber S, Maekawa H, Moreno-Borchart A, Doenges G, Schwob E, Schiebel E, Knop M (2004). A versatile toolbox for PCR-based tagging of yeast genes: new fluorescent proteins, more markers and promoter substitution cassettes. Yeast 21, 947–962.

Jimenez-Orgaz A, Kvainickas A, Nägele H, Denner J, Eimer S, Dengjel J, Steinberg F (2018). Control of RAB7 activity and localization through the retromer-TBC1D5 complex enables RAB7-dependent mitophagy. EMBO J 37, 235–254.

Klumperman J, Raposo G (2014). The complex ultrastructure of the endolysosomal system. Cold Spring Harb Perspect Biol 6, a016857.

Kvainickas A, Jimenez-Orgaz A, Nägele H, Hu Z, Dengjel J, Steinberg F (2017). Cargo-selective SNX-BAR proteins mediate retromer trimer independent retrograde transport. J Cell Biol 216, 3677–3693.

Liu TT, Gomez TS, Sackey BK, Billadeau DD, Burd CG (2012). Rab GTPase regulation of retromer-mediated cargo export during endosome maturation. Mol Biol Cell 23, 2505–2515.

Longtine M, McKenzie A, Demarini D, Shah N, Wach A, Brachat A, Philippsen P, Pringle J (1998). Additional modules for versatile and economical PCR-based gene deletion and modification in Saccharomyces cerevisiae. Yeast 14, 953–961.

Lucas M, Gershlick DC, Vidaurrazaga A, Rojas AL, Bonifacino JS, Hierro A (2016). Structural mechanism for cargo recognition by the retromer complex. Cell 167, 1623–1635.e14.

Peter BJ, Kent HM, Mills IG, Vallis Y, Butler PJG, Evans PR, McMahon HT (2004). BAR domains as sensors of membrane curvature: the amphiphysin BAR structure. Science 303, 495–499.

**Purushothaman LK, Arlt H,** Kuhlee A, Raunser S, Ungermann C (2017). Retromer-driven membrane tubulation separates endosomal recycling from Rab7/Ypt7-dependent fusion. Mol Biol Cell 28, 783–791.

Pylypenko O, Lundmark R, Rasmuson E, Carlsson SR, Rak A (2007). The PX-BAR membrane-remodeling unit of sorting nexin 9. EMBO J 26, 4788–4800.

Rojas R, van Vlijmen T, Mardones GA, Prabhu Y, Rojas AL, Mohammed S, Heck AJ, Raposo G, van der Sluijs P, Bonifacino JS (2008). Regulation of retromer recruitment to endosomes by sequential action of Rab5 and Rab7. J Cell Biol 183, 513–526.

Seaman M, Marcusson E, Cereghino J, Emr S (1997). Endosome to Golgi retrieval of the vacuolar protein sorting receptor, Vps10p, requires the function of the VPS29, VPS30, and VPS35 gene products. J Cell Biol 137, 79–92.

Seaman MNJ (2012). The retromer complex–endosomal protein recycling and beyond. J Cell Sci 125, 4693–4702.

Seaman MNJ, Gautreau A, Billadeau DD (2013). Retromer-mediated endosomal protein sorting: all WASHed up! Trends Cell Biol 23, 522–528.

Seaman MNJ, Harbour ME, Tattersall D, Read E, Bright N (2009). Membrane recruitment of the cargo-selective retromer subcomplex is catalysed by the small GTPase Rab7 and inhibited by the Rab-GAP TBC1D5. J Cell Sci 122, 2371–2382.

Simonetti B, Danson CM, Heesom KJ, Cullen PJ (2017). Sequence-dependent cargo recognition by SNX-BARs mediates retromer-independent transport of CI-MPR. J Cell Biol 216, 3695–3712.

Sorkin A, Zastrow von M (2009). Endocytosis and signalling: intertwining molecular networks. Nat Rev Mol Cell Biol 10, 609–622.

Stachowiak JC, Schmid EM, Ryan CJ, Ann HS, Sasaki DY, Sherman MP, Geissler PL, Fletcher DA, Hayden CC (2012). Membrane bending by protein-protein crowding. Nat Cell Biol 14, 944–949.

Steinberg F, Gallon M, Winfield M, Thomas E, Bell AJ, Heesom KJ, Tavaré JM, Cullen PJ (2013). A global analysis of SNX27–retromer assembly and cargo specificity reveals a function in glucose and metal ion transport. Nat Cell Biol 15, 1–13.

Strochlic TI, Setty TG, Sitaram A, Burd CG (2007). Grd19/Snx3p functions as a cargo-specific adapter for retromer-dependent endocytic recycling. J Cell Biol 177, 115–125.

van Weering JRT, Sessions RB, Traer CJ, Kloer DP, Bhatia VK, Stamou D, Carlsson SR, Hurley JH, Cullen PJ (2012a). Molecular basis for SNX-BAR-mediated assembly of distinct endosomal sorting tubules. EMBO J 31, 4466–4480.

van Weering JRT, Verkade P, Cullen PJ (2012b). SNX-BAR-mediated endosome tubulation is co-ordinated with endosome maturation. Traffic 13, 94–107.

Varandas KC, Irannejad R, Zastrow von M (2016). Retromer endosome exit domains serve multiple trafficking destinations and regulate local G protein activation by GPCRs. Curr Biol 26, 3129–3142.